Paper No. 594. (quote when citing this article)
Eleventh World Conference on Earthquake Engineering
ISBN: 0 08 042822 3

EXPERIMENTAL STUDY ON ULTIMATE HOLIZONTAL STRENGTH OF BUILDINGS SUPPORTED BY PILES

Y. NAGATAKI[1], K. AOSHIMA[1], H. HASHIZUME[1] and K. MORITA[2]

1)Technology Research Center TAISEI Corporation,
344-1 ,Nase-cho, Totsuka-ku,Yokohama 245, JAPAN
2) Department of Architecture ,Faculty of Engineering , University of Chiba,
1-33 ,Yayoi-cho, Inage-ku ,Chiba, 263, JAPAN

ABSTRACT

Three types of building models were tested by horizontal loading to investigate the collapse mechanism of the models. Type 1: fixed on rigid base. Type 2: supported by piles in a very weak soil model . Type 3: supported by piles in a weak soil model .For Type 1, all beam and column edges yielded up to the plastic strength of 34.3kN as the testing result. For Type 2, the pile heads and edges of footing beams yielded at the plastic strength of 16.7kN. For Type3, pile heads , edges of footing beams and edges of members yielded at the plastic strength of 30.4kN. Nonlinear analysis for the models with and without soil springs were carried out to compare with the test results. Experimental results were simulated very well by this analysis for Type 1. For Type 2 and 3 , results of analysis showed good agreement with experimental results for the load-deflection relationship .

KEYWORDS

Building supported by piles; Ultimate strength; Lateral loading test; Nonliner analysis; Kaolin clay

INTRODUCTION

The object of this study is to experimentally determine the collapse mechanism of the ground, pile and building system during the application of seismic force, and to prepare a non-linear model of the piles and ground in order to create an additional non-linear analytical model of upper structures.
With this in mind, lateral loading tests were conducted in order to gain an understanding of the differences between collapse mechanisms during application of seismic lateral force for three cases: (1) the upper structure collapses, (2) the support piles primarily collapse, and (3) the combined collapse of the upper structure and support piles occur. In addition, a ground-pile-building composite model was prepared that took into consideration gaps that form between the ground and piles to examine the applicability of the analytical method by comparing analytical and experimental results.

EXPERIMENT SUMMARY

Setting of Target Building

A five-story reinforced concrete building supported by piles and standing on soft ground was set for a reference as the target building for preparing the model test building. The piles consisted of cast-in-place concrete piles (ϕ 1250 mm), and the depth of the upper surface of the support layer was G.L. -19 m. Furthermore, a two-story building was used as the test building due to restrictions on the experimental apparatus.

Law of Similarity

The basis similarity ratio was taken to be the similarity ratio between length and stress. The similarity ratio of length was set at 1/10 while that of stress was set at 1.0. The similarity ratios of other physical quantities were determined by deriving from the basic similarity ratio.
Incidentally, the similarity ratio for the deformation modulus of the ground was set as indicated below in accordance with the technique of Tominaga, *et al.*, 1986.

Table 1. Similarity ratio

Items	Symbol	Dimension	Similarity Ratio	Scale
Length	L	L	$1/\lambda$	1/10
Density	ρ	FL^{-3}	1	1
Weight, Force	F	F	$1/\lambda^2$	1/100
Modulus of Elasticity	E	FL^{-2}	1	1
Poisson's ratio	ν	–	1	1
Inertia Moment	I	L^4	$1/\lambda^4$	1/10000
Bending Rigidity	EI	FL^2	$1/\lambda^4$	1/10000
Bending Moment	M	FL	$1/\lambda^3$	1/1000
Displacement	δ	L	$1/\lambda$	1/10
Stress	σ, τ	FL^{-2}	1	1
Strain	ϵ, γ	–	1	1

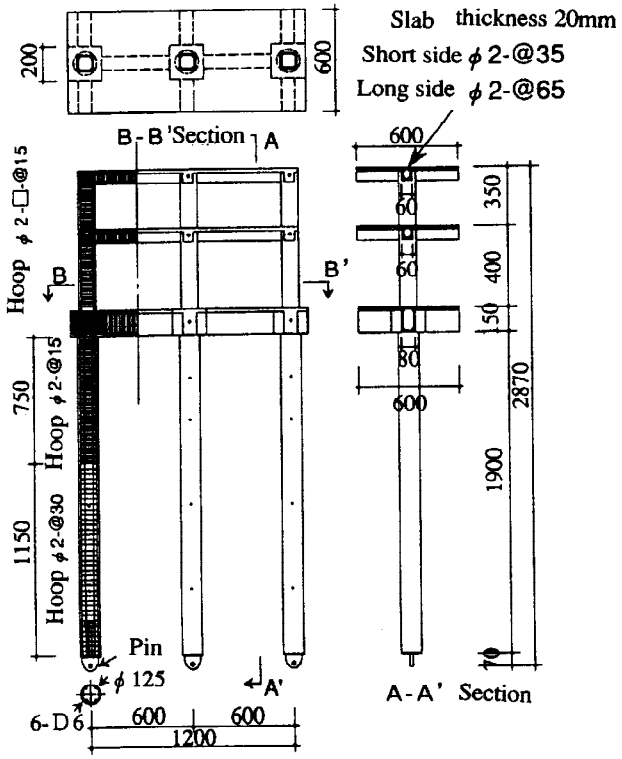

Fig. 1. Test Spacimen (Type 3)

Table 2. Relation ship between building and model

			Original	Scale	Model
Super structure	2nd,RF's Beam size (cm)		60×80	1/10	6×8
	1st,2nd F's column size (cm)		100×100	1/10	10×10
	Foundation beam size (cm)		80×150	1/10	8×15
	Young's Modulus (kgf/cm^2)	Type1,2	1.82×10^5	1	1.82×10^5
		Type3	2.03×10^5	1	2.03×10^5
	Beam's bending rigidity ($kgf\,cm^2$)	Type1,2	4.66×10^{11}	1/10000	4.66×10^7
		Type3	5.20×10^{11}	1/10000	5.20×10^7
	Column's bending rigidity ($kgf\,cm^2$)	Type1,2	1.52×10^{12}	1/10000	1.52×10^8
		Type3	1.69×10^{12}	1/10000	1.69×10^8
	Foundation beam's bending rigidity ($kgf\,cm^2$)	Type2	4.10×10^{12}	1/10000	4.10×10^8
		Type3	4.57×10^{12}	1/10000	4.57×10^8
Pile	Pile's diameter (cm)		125	1/10	12.5
	Pile's length (cm)		1900	1/10	190
	Young's Modulus (kgf/cm^2)	Type2	1.68×10^5	1	1.68×10^5
		Type3	2.03×10^5	1	2.03×10^5
	Bending rigidity ($kgf\,cm^2$)	Type2	1.71×10^{12}	1/10000	1.71×10^8
		Type3	2.07×10^{12}	1/10000	2.07×10^8
Soil	Depth (cm)		1900	1/10	190
	Density (gf/cm^3)	Type2	1.5	1	1.3
		Type3	1.5	1	1.3
	Uniaxial strength (kgf/cm^2)	Type2	0.1	1	0.09
		Type3	0.4	1	0.38
	Young's Modulus (kgf/cm^2)	Type2	7.0	1	6.7
		Type3	90.0	1	90.9

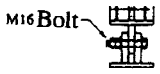

Detail of pin of end of pile

[Unit: mm]

The basic equation for elastic support beams is expressed by the following Equation (1).

$$E_p I_p (d^4y/dx^4) + \alpha E_s y = 0 \quad (1)$$

where,

E_p: Young's modulus of the model piles
I_p: Inertia moment of the model piles
y: Horizontal displacement of the model piles at depth x
x: Depth from the ground surface
E_s: Deformation modulus of model ground
α : Similarity ratio of deformation modulus of model ground

In considering the original piles, since $I_p = 10^4$ times and x and y = 10 times, the similarity ratio a of the deformation modulus of the model ground is 1. That is, there should be prepared a model ground having the same deformation modulus as that of the original ground.
Similarly, the uniaxial compressive strength of the model ground is equal to that of the original ground. Similarity ratios are summarized in Table 1.

Test Building Fixed on a Rigid Base (Type 1)

In order to make the upper structure equivalent to the test building supported by piles described in section 2.4 (Type 2) and increase the rigidity of the pedestal, the building was not fixed on footing beams but rather on a mass concrete foundation (1660 x 500 x 150).

Test Building Supported by Piles (Types 2 and 3)

The reinforcing bar arrangement drawing of the test building supported by piles (Type 3) is shown in Fig. 1. The arrangement of bars was determined according to the law of similarity from the reinforcing bar cross-sectional surface area of the original building. It should be noted that Type 2 is not provided with a slab for the purpose of simplification. In addition, mortar and not concrete is used to reduce the size of the test buildings. Table 2 provides a summary of the relationship between the original building and test buildings. The cross-sectional shapes and cross-sectional performances of each member are shown in Table 3.

Model Ground

The blending ratios of the model ground for the test buildings of types 2 and 3 were set such that the uniaxial compressive strengths of the model ground were 9.8 kPa and 29.4 kPa, respectively. Furthermore, block sampling was performed at a pitch of 50 cm in depth from the model ground for the type 2 test building and from the surface layer only for the type 3 test building following the lateral loading test. Uniaxial compression tests were then performed using those samples. Those test results are shown in Table 4.

Loading Method

The column axial force for the type 3 test building supported by piles was 19.6 kN at the central column and 9.8 kN at the columns on both edges. Long-term axial force in the vertical direction was not applied to the type 1 test building fixed on a rigid base or to the type 2 test building supported by piles.
While in the state described above, lateral loading was performed repeatedly using two hydraulic jacks. The load distribution for all three types of test buildings was taken to be inverted triangular distribution having an RF:2F of 2:1. The loading apparatus is shown in Fig. 2, while the loading cycle is illustrated in Fig. 3. Incidentally, the final loading was applied so that the plasticity index exceeded 4.

Table 3. Properties of members

Member		Section size b×D (mm)	Crack Moment Mc (N · cm)	Yield Moment My (N · cm)
2,RF Beam	Type1,2	60×80	21139	162004
	Type3	60×80	42728	21979 (Upper Tension) 162004 (Lower Tension)
1,2F Column		100×100	55047	205722
Foundation Beam	Type1,2	80×150	99088	324008
	Type3	80×150	141933	411326 (Upper Tension) 324008 (Lower Tension)
Pile		ϕ 125	56223	355123

Table 4. Material properties of soils

Depth (cm)		Unit volume weight γ (kN/m^3)	Uniaxial compressive strength qu (kPa)	Ground deformation modulus Eo (kPa)
Type2	GL-10	12.3	6.86	613.5
	GL-50	12.2	6.86	513.5
	GL-100	12.3	7.84	363.6
	GL-200	12.4	8.82	659.5
Type3	GL-10	12.8	37.2	8908.2

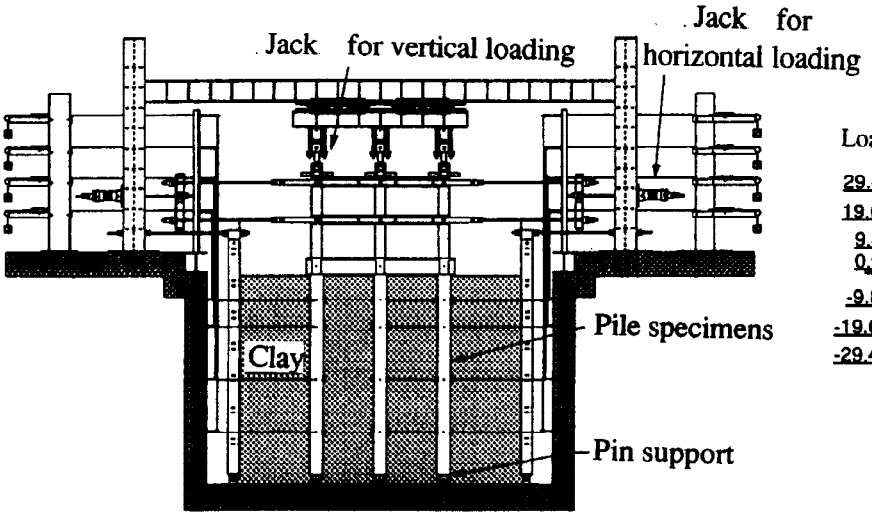

Fig. 2. Loading apparatus

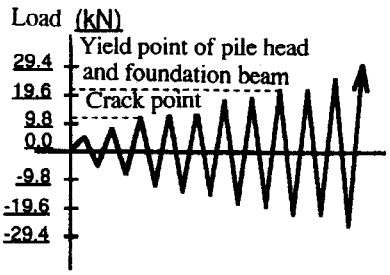

Fig. 3. Loading cycle

Measurement Methods

The horizontal displacement of the 2nd floor and roof along with the strain of the beams and major reinforcing bars of the column edges were measured for the test building fixed on a rigid base (Type 1). The horizontal displacement of the foundation, 2nd floor and roof along with the strain of the beams, columns and major bars of the piles were measured for the test building supported by piles on very weak soil (Type 2). In the case of the test building supported by piles on weak soil (Type 3), in addition to the measurements for Type 2, the vertical displacement of the four corners of the foundation, the earth pressure of the piles and the displacement from the ground surface at depths of 25, 50, 100 and 150 cm were also measured.

ANALYSIS BY LOAD INCREMENTATION

Analysis Method

Analysis was performed according to the load incrementation method using the test building supported by piles and the test building fixed on rigid base shown in Fig. 4 as the analysis models.
Two types of loading were employed consisting of unidirectional monotoneous loading and repeated loading. The axial strength and expansion of the piles were taken into consideration for monotoneous loading, while the axial

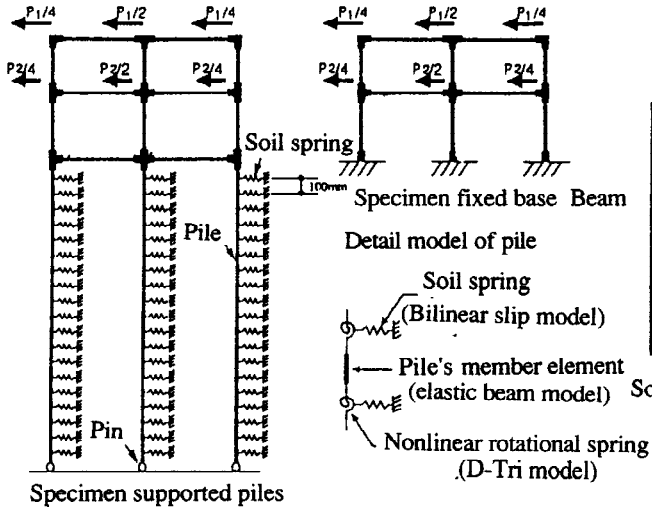

Fig. 4. Analytical model

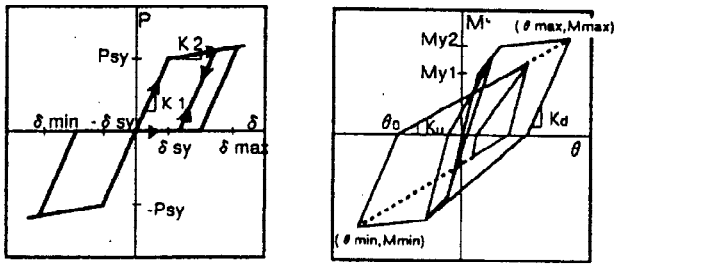

Fig. 5. Hysteresis models of soil and rotational spring

strength was taken to be 0 in the case of repeated loading without considering fluctuating axial strength and pile expansion.
Models of column, beam and pile members were prepared with beam elements having plastic rotational springs on both ends to consider only bending failure. The D-Tri type (Umemura, 1973) was used as the reversion strength model of the plastic rotational springs.
A bilinear slip type was used as the ground reversion strength model since reversion strength properties are of the hard spring type due to the formation of a gap between the piles and ground. A model was therefore created with a horizontal spring. Fig. 5 shows the reversion strength models of the ground spring and plastic rotational spring.

The spring constant of the ground was determined using Equations (2) and (3), while ultimate strength Nu was calculated from the Rankine-Lezarre equation (K. Terzaghi, 1969). In this analysis, in order to express the reversion strength of the ground in the form of bilinear slip, the first slope of spring rigidity of the ground was calculated using E_{70} of the results of the uniaxial compression strength test, while that for the second slope was calculated using the slope of the straight line that connects q_{70} and q_u. At this time, the reduction coefficient a for determining the secondary slope was 0.1. Here, q_{70} is a value equal to 70% of q_u, while E_{70} is the slope that connects q_{70} and the origin.

$$K_1 = K_h B l \quad (2)$$
$$K_2 = \alpha K_1 \quad (3)$$

where,
K_1, K_2: Spring rigidity of ground (1st slope, 2nd slope)
K_h: Horizontal ground reaction coefficient $[=0.8E_0B^{-3/4}]$,E_0 = Ground deformation modulus
B: Pile diameter ,l: Distance between supporting points of ground spring (100mm pitch)
α : Reduction coefficient ($\alpha = 0.1$)

$$P_{sy} = 0.7N_u \quad (4)$$

where,
P_{sy}: 70% of ultimate strength of ground (bilinear bending point)
N_u: Ultimate strength of ground $[=(q_u + K_p \gamma h)Bl]$
q_u: Uniaxial compressive strength of ground
K_p: Coefficient of passive earth pressure $[=\tan^2(45°+ \phi /2)]$, ϕ : Angle of internal friction ($\phi = 0$)
γ : Unit volume weight of soi , h: Depth of location of ultimate strength to be determined

The cracking moment and yield moment of columns and beams were calculated using Equations (5) through (8). Slab effects were also taken into consideration for the test building supported by piles on weak ground (Type 3). Yield moment of pile members was determined based on the bending strength determination method for cast-in-place piles using the e function method (Japan Construction Association, 1976).

$$CMc = 2\sqrt{Fc}Z + ND/6 \quad (5)$$
$$CMy = 0.8at\ \sigma\ yD + 0.5ND\{1-N/(bDFc)\} \quad (6)$$
$$GMc = 2\sqrt{Fc}Z \quad (7)$$
$$GMy = 0.9at\ \sigma\ yd \quad (8)$$

where,
CMc: Cracking moment of columns, CMy: Yield moment of columns ,GMc: Cracking moment of beams
GMy: Yield moment of beams ,Fc: Concrete strength,, N: Axial strength ,Z: Section modulus
D: Total column length ,d: Effective length, ,b: Column width
at: Tensile reinforcing bar cross-sectional surface area , σ y: Unit tensile stress of reinforcing bars

Comparison of Hysteresis Characteristic

Figs. 6 and 7 indicate the relationship between story-shearing force and inter-story displacement of the 1st floor of the test building supported by piles on very weak ground (Type 2) along with a comparison of experimental results and repetitive analytical results for the relationship between foundation shearing force and absolute displacement. Moreover, analytical results obtained by monotoneous loading are indicated by a dotted line in the experimental results.
Analytical results of unidirectional monotoneous loading closely coincided with experimental results with respect to the relationship between story-shearing strength and inter-story displacement of the 1st floor of the Type 2 test building. While repetitive analytical results closely coincided with experimental results for maximum shearing strength, inter-story displacement was roughly half that of the experimental results, and experimental results for rigidity were lower than those of the analytical results. One possible cause of this is that, although the rotational

displacement component resulting from elongation of the piles is included in the horizontal displacement measured in the experiments, the horizontal displacement caused by this rotation is not considered in the analytical results.

In looking at the relationship between shearing force and displacement of the foundation on the test building supported by piles on very weak ground (Type 2), the relationship closely coincides with the envelope up to the maximum load in the analytical results for monotoneous loading, and it tends to increase beyond that point. This is considered to be the result of the ground reversion strength model also having a slope beyond the ultimate strength of the ground.

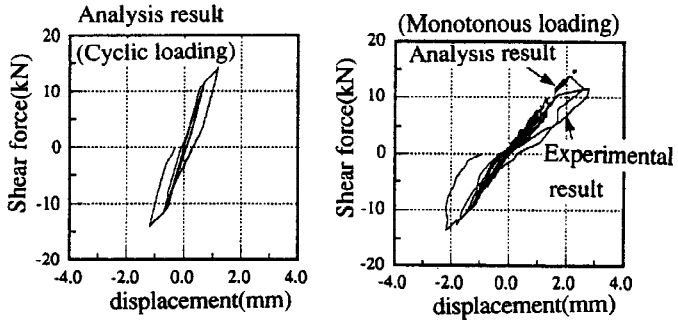

Fig. 6. Shear force-dehlection relationship (Type2 1st. Floor)

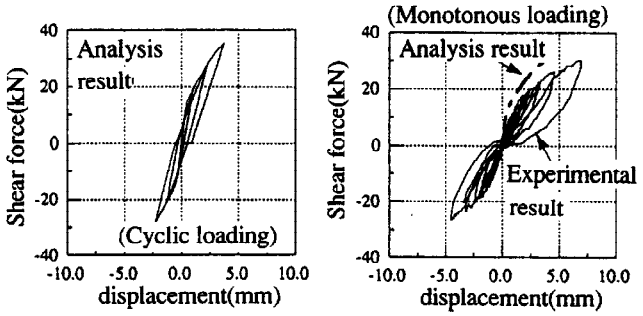

Fig. 8. Shear force-dehlection relationship (Type3 1st. Floor)

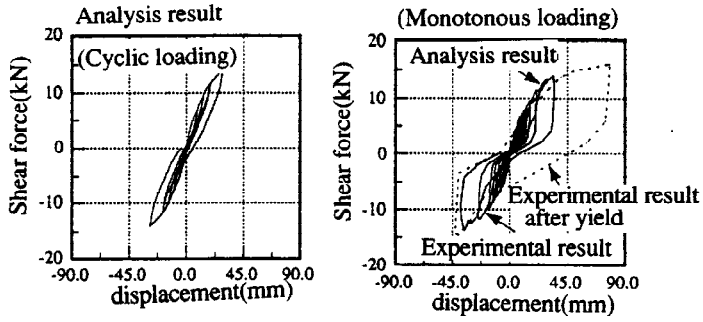

Fig.7. Shear force-dehlection relationship (Type2 Foundation)

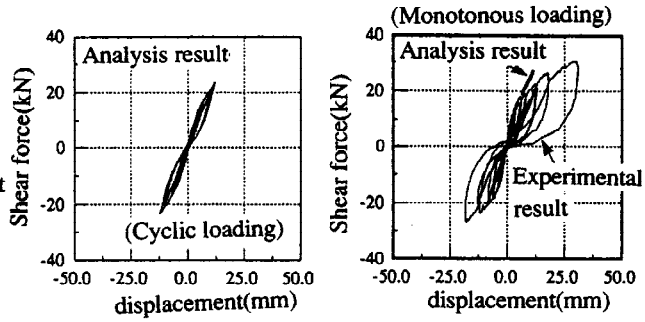

Fig.9. Shear force-dehlection relationship (Type3 Foundation)

According to the results of repetitive analysis, the envelope of shearing strength and hysteresis loop during maximum displacement in the analysis closely coincided with experimental results. However, when the skeleton curve of each loop is examined closely, experimental results indicate that after a gap is formed between the ground and piles, reversion strength properties take on the form of a hard spring (inverted S type) due to the effects of this gap closing when force in the opposite direction is applied. Although these effects are demonstrated to a certain extent in the analytical results as well, they are not significant.

The relationship between story-shearing force and inter-story displacement of the 1st floor of the test building supported by piles on weak ground (Type 3) is shown in Fig. 8, while the relationship between shearing strength and displacement of the foundation is shown in Fig. 9. In addition, analytical results for unidirectional monotoneous loading are also shown in the experimental results in the same manner as the Type 2 test building. As can be seen in Fig. 9, the analytical results for monotoneous loading closely coincide with the envelope up to about 19.6 kN, there is a tendency to increase beyond that point. This is considered to be the result of the reversion strength properties of the ground model having a slope that extends beyond ultimate strength, as previously mentioned.

Repetitive analytical results were unable to be calculated through the final loop due to the results having a lack of convergence and diverging during large deformation, but in looking at results up to about yielding of the pile heads prior to reaching large deformation, maximum strength and hysteresis loop surface area nearly coincide. In addition, although reversion strength properties according to the analytical results are in the form of a hard spring, it is not remarkable.

Comparison of Bending Moment Distribution

The bending moment distribution during footing beam yielding (during application of a force of 14.0 kN) for the test building supported by piles on very weak ground (Type 2) as well as that during footing beam and pile top yielding (during application of a force of 20.6 kN) for the test building supported by piles on weak ground (Type 3) are shown in Fig. 10. The bending moments shown in this diagram assume plane retention are calculated using the strain of the tops and bottoms of members in the case of beams, and the strain of the major bars of the left and right edges in the case of columns and piles. The black dots ● in the diagram indicate the locations of initial yielding. In the test building supported by piles on very weak ground (Type 2), the bending moment of the right edge of the right footing beam reaches a maximum. In addition, the bending moment of the piles is largest at the pile heads in comparison with the underground portions, and is distributed such that it decreases nearly positively as depth increases.

The bending moment of the test building supported by piles on weak ground (Type 3) is such that the bending moment of the pile heads of the central piles tends to be larger than those of the piles on both sides. In addition, bending moment distribution of underground portions differs from that of the Type 2 test building in that, although bending moment is distributed positively near the pile heads, it reaches a maximum underground after changing to a negative distribution as depth increases after which it again decreases. In addition, the pile heads of the central piles as well as the bars of the upper end of the right edge of the right footing beams yielded simultaneously at this time.

Fig. 11 indicates a comparison of bending moment distribution for the test building supported by piles on very

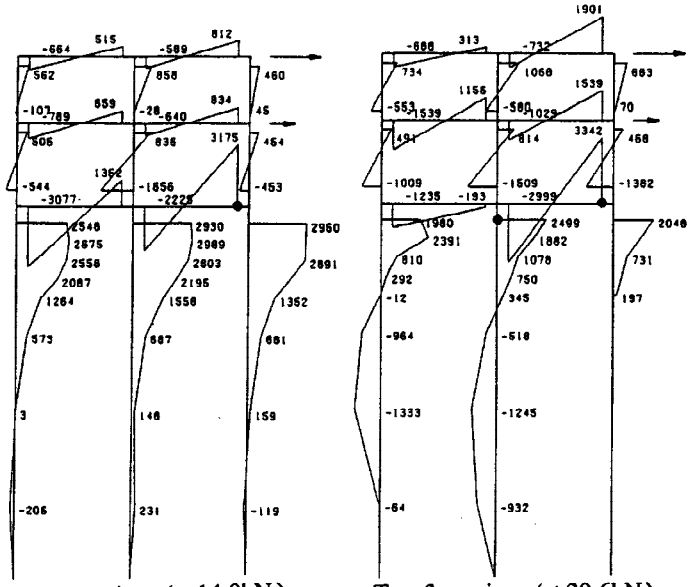

Fig. 10. Bending moment distribution [Unit : Nm] (Experiment)

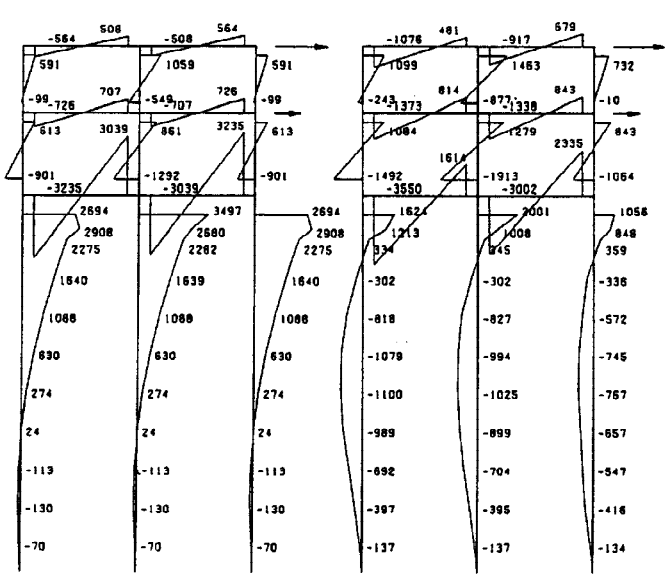

Fig. 11. Bending moment distribution [Unit : Nm] (Analysis)

weak ground (Type 2) when applying a force of 14.0 kN, and for the test building supported by piles on weak ground (Type 3) when applying a force of 20.6 kN as obtained from repetitive analytical results.

In the test building supported by piles on very weak ground (Type 2), the bending moment of the pile heads of the central piles is the largest, and tends to decrease positively as depth increases.

In the test building supported by piles on weak ground (Type 3), bending moment is different. Namely, although the distribution is positive at the pile heads, distribution changes over to a negative distribution as depth increases, after which it decreases. In addition, although the magnitude is slightly different, this distribution coincides with the form of bending moment distribution of the piles in the experimental results shown in Fig. 10.

Comparison of Order of Yield

Fig. 12 illustrates a comparison of experimental results and repetitive analytical results for yield order of each of the test buildings. The black dots in the diagram indicate the order of yield as determined by considering yield to have occurred when the major bars of the upper or lower end yielded in the case of beams, and when either the left or right major bars yielded in the case of columns.

In the test building fixed on a rigid base (Type 1), analytical results indicate a failure process in which the 1st floor

pedestal portion yielded first, followed by the beam ends and finally the column ends of the 2nd floor and roof. These results closely coincided with experimental results.

In the test building supported by piles on very weak ground (Type 2), experimental results indicated a failure process in which the right edge of the right footing beams yielded first, followed by the left edge of the left footing beams and finally the area in the vicinity of the pile tops of the right and central piles. On the other hand, analytical results indicated a failure process wherein the outer edges of the respective footing beams yielded first, followed by the pile tops of the central piles and finally all edges of the footing beams.
In the test building supported by piles on weak ground (Type 3), the pile heads of the central piles yielded first according to both experimental and analytical results. However, in contrast to the next location of yielding being the right edges of the footing beams according to experimental results, the next location according to analytical results is the pile tops of the left and right piles.
The following provides an explanation of some possible causes of the discrepancies in the order of pile yield between experimental and analytical results.

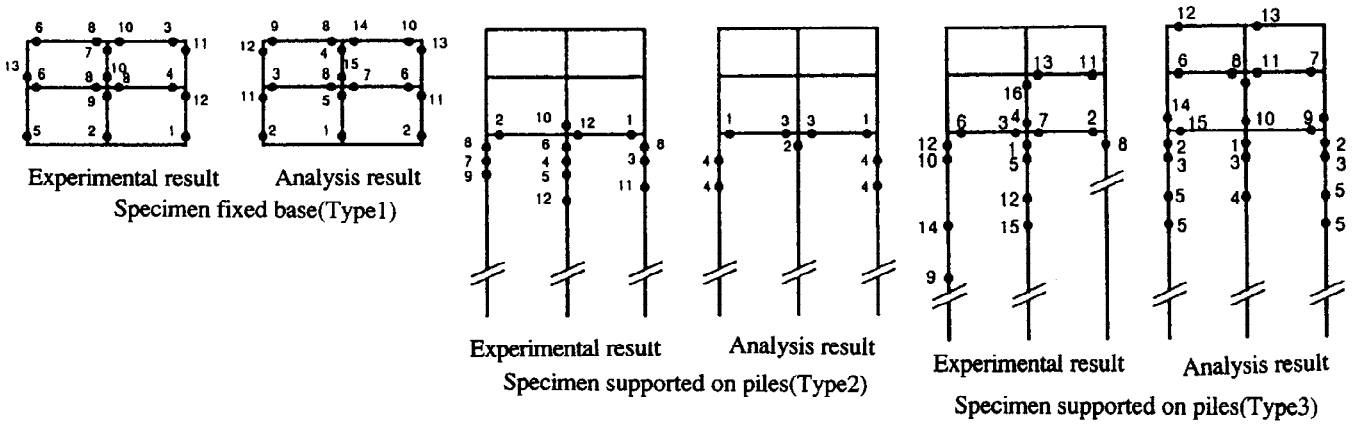

Fig. 12. Yielding order main reinforced bar

With respect to the test building supported by piles on very weak ground (Type 2), since force was applied by pulling on the upper structure in the experiment, tensile or compressive axial force was produced in the outer piles. Consequently, the yield bending moment of the outer piles in which tensile axial force was produced decreased, thus making them more susceptible to yielding.
On the other hand, with respect to analytical results, since changes in bending strength accompanying fluctuating axial strength of the piles were not taken into consideration, the central piles were considered to have yielded first since they have a larger bending moment as compared with the right and left piles. In addition, with respect to the test building supported by piles on weak ground (Type 3), since long-term axial force together with fluctuating compressive force were applied to the outer piles in the experiment, the yield bending moment of the piles became larger. In the analysis, however, the pile heads were considered to have yielded first since this fluctuating compressive force was not taken into consideration.

CONCLUSION

The analytical results of unidirectional monotoneous loading coincided with the envelope of experimental results up to the ultimate strength of the ground for both Types 2 and 3. Simulations using repetitive plasticity analysis were conducted on the test building supported by piles (Types 2 and 3). As a result, the envelope of the hysteresis loop nearly coincided with experimental results up to 30 mm for Type 2 and up to 13 mm for Type 3.

REFERENCES

K. Tominaga, H. Yamamoto and T. Somekawa (1986): Model Experimentation on the Horizontal Behavior of Pile Groups Subjected to Vertical Force, *The Structural Department of the Japan Construction Association*, No. 394, pp. 130-139.

K. Umemura (1973): *Dynamic Aseismic Design of Reinforced Concrete Structures*,(Gihodo Publishing), pp. 286-288.

Terzaghi and Peck (1987): *Soil Mechanics*, (Maruzen Publishing), pp. 172-173.

Japan Foundation Construction Association (1976): Calculation of Horizontal Strength of Cast-in-Place Concrete Piles, pp. 56-57.